JCI insight

Circumventing cellular immunity by miR142-mediated regulation sufficiently supports rAAV-delivered OVA expression without activating humoral immunity

Yuanyuan Xiao, … , Phillip W.L. Tai, Guangping Gao

JCI Insight. 2019;4(13):e99052. https://doi.org/10.1172/jci.insight.99052.

Research Article | Immunology | Therapeutics

Recombinant adeno-associated virus–mediated (rAAV-mediated) gene delivery can efficiently target muscle tissues to serve as “biofactories” for secreted proteins in prophylactic and therapeutic scenarios. Nevertheless, efficient rAAV-mediated gene delivery is often limited by host immune responses against the transgene product. The development of strategies to prevent antitransgene immunity is therefore crucial. The use of endogenous microRNA-mediated (miRNA-mediated) regulation to detarget transgene expression from antigen-presenting cells (APCs) has shown promise for reducing immunogenicity. However, the mechanisms underlying miRNA-mediated modulation of antitransgene immunity by APC detargeting are not fully understood. Using the highly immunogenic ovalbumin (OVA) protein as a proxy for foreign antigens, we show that rAAV vectors containing miR142-binding sites efficiently repress costimulatory signals in DCs, significantly blunt the cytotoxic T cell response, allow for sustained transgene expression in skeletal myoblasts, and attenuate clearance of transduced muscle cells in mice. Furthermore, the blunting of humoral immunity against circulating OVA correlates with detargeting of OVA expression from APCs. This demonstrates that incorporating APC-specific miRNA-binding sites into rAAV vectors provides an effective strategy for reducing transgene-specific immune response. This approach holds promise for clinical applications where the safe and efficient delivery of a prophylactic or therapeutic protein is desired.

JCI insight

RESEARCH ARTICLE

Circumventing cellular immunity by miR142-mediated regulation sufficiently supports rAAV-delivered OVA expression without activating humoral immunity

Yuanyuan Xiao,[1,2,3] Manish Muhuri,[2,3] Shaoyong Li,[2,3] Wanru Qin,[1] Guangchao Xu,[1,2,3] Li Luo,[1,2,3] Jia Li,[2,3] Alexander J. Letizia,[4,5] Sean K. Wang,[5] Ying Kai Chan,[4,5] Chunmei Wang,[1] Sebastian P. Fuchs,[6] Dan Wang,[2,3] Qin Su,[2] M. Abu Nahid,[2,3] George M. Church,[4,5] Michael Farzan,[7] Li Yang,[1] Yuquan Wei,[1] Ronald C. Desrosiers,[6] Christian Mueller,[2,8,9] Phillip W.L. Tai,[2,3] and Guangping Gao[2,3,9]

[1]State Key Laboratory of Biotherapy and Cancer Center, West China Hospital, Sichuan University, and Collaborative Innovation Center for Biotherapy, Chengdu, China. [2]Horae Gene Therapy Center and [3]Department of Microbiology and Physiological Systems, University of Massachusetts Medical School, Worcester, Massachusetts, USA. [4]Wyss Institute for Biologically Inspired Engineering, Harvard University, Boston, Massachusetts, USA. [5]Department of Genetics, Harvard Medical School, Boston, Massachusetts, USA. [6]Department of Pathology, University of Miami Miller School of Medicine, Miami, Florida, USA. [7]Department of Infectious Diseases, The Scripps Research Institute, Jupiter, Florida, USA. [8]Department of Pediatrics and [9]Li Weibo Institute for Rare Diseases Research, University of Massachusetts Medical School, Worcester, Massachusetts, USA.

Recombinant adeno-associated virus–mediated (rAAV-mediated) gene delivery can efficiently target muscle tissues to serve as "biofactories" for secreted proteins in prophylactic and therapeutic scenarios. Nevertheless, efficient rAAV-mediated gene delivery is often limited by host immune responses against the transgene product. The development of strategies to prevent antitransgene immunity is therefore crucial. The use of endogenous microRNA-mediated (miRNA-mediated) regulation to detarget transgene expression from antigen-presenting cells (APCs) has shown promise for reducing immunogenicity. However, the mechanisms underlying miRNA-mediated modulation of antitransgene immunity by APC detargeting are not fully understood. Using the highly immunogenic ovalbumin (OVA) protein as a proxy for foreign antigens, we show that rAAV vectors containing miR142-binding sites efficiently repress costimulatory signals in DCs, significantly blunt the cytotoxic T cell response, allow for sustained transgene expression in skeletal myoblasts, and attenuate clearance of transduced muscle cells in mice. Furthermore, the blunting of humoral immunity against circulating OVA correlates with detargeting of OVA expression from APCs. This demonstrates that incorporating APC-specific miRNA-binding sites into rAAV vectors provides an effective strategy for reducing transgene-specific immune response. This approach holds promise for clinical applications where the safe and efficient delivery of a prophylactic or therapeutic protein is desired.

Authorship note: YX, MM, and SL contributed equally to this work.

Conflict of interest: GG is a cofounder of Voyager Therapeutics and Aspa and holds equity in these companies. GG is an inventor on patents (PCT/US2015/027591) with potential royalties licensed to Voyager Therapeutics, Aspa, and other biopharmaceutical companies. CM is a cofounder of Apic Bio and holds equity in the company. CM is an inventor on patents with potential royalties licensed to Apic Bio. YKC and GMC are cofounders of Ally Therapeutics. GMC is a founder of Editas Medicine and eGenesis Bio (for the full disclosure list, please see http://arep.med.harvard.edu/gmc/tech.html).

Submitted: December 6, 2017
Accepted: May 16, 2019
Published: July 11, 2019.

Reference information: *JCI Insight*. 2019;4(13):e99052. https://doi.org/10.1172/jci.insight.99052.

Introduction

Skeletal muscle is an attractive target tissue for the exogenous production and secretion of prophylactic and therapeutic agents against infectious diseases (1). Recombinant adeno-associated viruses (rAAVs) are among the most promising gene transfer vehicles for many therapeutic applications (2). Numerous studies have shown that rAAV can deliver and express genes in a wide variety of tissues, including muscle (3). Preclinical and clinical evidence has demonstrated that rAAV can mediate persistent and long-term expression of transgenes with few side effects (4). Recently, the utility of rAAV has been expanded to include the exogenous expression of broadly neutralizing antibodies or modified CD4-Igs for preventing infectious diseases such as AIDS (5–8), hepatitis C (9), malaria (10), and influenza (11). However, a major limitation to these approaches has been the development of immune responses to prophylactic and therapeutic

transgene products when delivered by rAAVs. Specifically, antigen-specific B cell activation results in the production of inhibitory antibodies against transgene products, thereby impairing treatment potential. In recent studies, these anti-antibody responses were observed in macaques (6, 7). In addition, adeno-associated virus–mediated (AAV-mediated) gene delivery can lead to transgene-specific cellular immunity (12) or even trigger autoimmunity toward endogenous proteins (13, 14).

A well-known cause for transgene-related immunotoxicity is the undesirable transduction of antigen-presenting cells (APCs), which in turn triggers host immunity toward rAAV-expressed transgene products (15, 16). Among professional APCs (e.g., DCs, macrophages, and B lymphocytes), DCs may represent the most important cell type in the host, having the broadest range of antigen presentation. Therefore, rAAV transduction of DCs can lead to the display of transgene peptide epitopes on MHC class I molecules. Such events would in turn activate cytotoxic $CD8^+$ T lymphocytes (CTLs) to clear cells that express the exogenous protein. Undesirable transgene expression in DCs can be potentially overcome by the use of highly specific tissue promoters. However, rAAV-compatible, muscle-specific regulatory cassettes derived from the Desmin promoter or the synthetic C5-12 promoter have been shown to be leaky in DCs (17, 18). Therefore, alternative strategies to effectively reduce spurious expression in DCs may help attenuate transgene-related immune responses following rAAV transduction.

miRNAs are small, noncoding RNAs that regulate gene expression by posttranscriptional silencing (19). When miRNAs are partially complementary to the target mRNA sequence, they typically reduce target mRNA stability and inhibit translation (20). In contrast, when miRNAs exhibit near-perfect complementarity to their targets, they trigger degradation of the mRNA via Ago2 cleavage (20). The use of miRNA-binding sites for cell type–specific detargeting to attenuate transgene immunogenicity was first described using lentiviral vectors to suppress transgene expression in different hematopoietic lineages (21, 22). miRNA-mediated detargeting can also be used to assist tissue-specific expression by posttranscriptional control to restrict spuriously transcribed transgenes that result from the wide transduction profiles of rAAVs (23–26). Many miRNAs have been reported to be involved in the regulation and development of macrophages, DCs, and B cells (27–29). Among these, miR-142 is regarded as a hematopoietic-specific miRNA (21, 30) and, as such, is expressed in APCs. A previous report demonstrated that miR-142–binding sites (miR142BSs) that were inserted into the 3′-UTR of the highly immunogenic *OVA* cDNA (17) were sufficient in preventing transgene immunity when delivered by rAAV while maintaining expression in muscle. Although these previous studies demonstrated promising results for attenuating transgene immunity, the utility for miR-mediated detargeting has been shown to be context dependent. Namely, Boisgerault et al. reported that the use of miR-142-3p–targeted sequences was able to attenuate transgene immunity in normal C57BL/6 mice but not in the *Sgca*$^{-/-}$ muscular dystrophy mouse model that is deficient in α-sarcoglycan (18). Thus, further investigation into the nature of miR-142 detargeting is warranted. Here, we present evidence that the mechanism for APC-specific attenuation of transgene immunity by miRNA-mediated regulation involves circumventing cell-mediated immunity via the inhibition of cytotoxic CTLs. Humoral immunity is found to be less of a contributing factor once the CTL response is overcome and levels of secreted transgene product are elevated in the circulation. Detargeting mediated by miR-142 can also serve as a robust strategy to suppress immune responses against redosing with a different vector serotype that expresses the same transgene product given at the first dose, effectively boosting its therapeutic potential. These findings demonstrate that posttranscriptional regulation through miRNA binding is a robust method for overcoming transgene immunity toward secreted proteins, thereby improving the efficacy and safety of prophylactic and therapeutic gene delivery.

Results

Engineering of miR142BSs within the OVA 3′-UTR leads to repressed expression of OVA in DCs and macrophage cells but not in myoblasts. To explore the functionality of miR-142–mediated APC detargeting of a foreign transgene, 2 copies of miR142BSs were engineered into the 3′-UTR of the highly immunogenic *OVA* cDNA, a design similar to those previously reported by others (31). To achieve persistent promoter activity, the strong and ubiquitous CMV enhancer/chicken β-actin promoter (32) was selected to express OVA instead of the CMV promoter because it has been shown that CMV-driven transgene expression tends to be silenced in certain cell types in vitro and in vivo (33). *Ova* constructs were then subcloned into rAAV vectors (Figure 1A). To demonstrate the efficacy of the miR142BS element to detarget OVA expression in immune cells while maintaining muscle expression, we chose to use mouse immature DCs (JAWS II),

mouse macrophage cells (RAW264.7), and the mouse C2C12 skeletal myoblast cell line. Endogenous levels of miR-142-3p in JAWS II and RAW264.7 were found to be approximately 400- and 600-fold higher than in C2C12 cells, respectively (Figure 1B). Plasmids carrying OVA with miR142BS (OVA.miR142BS) or without the element were transfected into these cell lines, and levels of secreted OVA were then measured in the respective cell culture supernatants 72 hours after transfection (Figure 1C). Notably, the inherent differences in transfection efficiencies and transgene promoter activities in different cell types likely contribute to the variance of detectable OVA between cell lines. Importantly, cells transfected with OVA.miR142BS resulted in nearly undetectable levels of OVA secreted from JAWS II and RAW264.7 cells. C2C12 cells that were transfected with OVA.miR142BS exhibited similar levels of secreted OVA as compared with C2C12 cells that were transfected with an OVA construct lacking the miR142BS (Figure 1C). In addition, exogenous expression of OVA transcripts carrying the miR142BS element does not alter endogenous miR-142-3p mRNA expression (Supplemental Figure 1; supplemental material available online with this article; https://doi.org/10.1172/jci.insight.99052DS1).

rAAV1-OVA.miR142BS transduction of skeletal muscle tissues leads to stable OVA expression with a negligible anti-OVA antibody response. We next aimed to determine the influence of miR142BS-mediated detargeting on transgene-specific B cell response in muscle tissue in vivo. Among AAV serotypes evaluated for muscle-directed gene transfer, intramuscularly delivered AAV1 stands out for its highly efficient and localized transduction of skeletal muscle, its limited systemic biodistribution, and its history of use in human muscle for the ectopic expression of therapeutic proteins (34–36). Importantly, it has also been shown to transduce APCs to elicit transgene immunity (31). We therefore packaged rAAV.OVA with or without the miR142BS element into AAV1 capsids and injected these vectors into tibialis anterior (TA) muscles of adult mice. Two weeks after intramuscular (i.m.) delivery, the levels of vector genomes detected in the muscle were high, while levels were relatively low in the spleen, heart, and liver (Figure 2A). Interestingly, we observed a 3-fold higher abundance of genomes in muscles treated by rAAV1.OVA.miR142BS vectors. Serum levels of OVA and anti-OVA antibodies were then measured over the course of 12 weeks (Figure 2, B and C). Animals injected with rAAV1.OVA.miR142BS vectors generated high and sustained levels of OVA expression in the circulation, with a negligible anti-OVA antibody response (IgG1). In contrast, animals treated with rAAV1.OVA lost all detectable levels of OVA 4 weeks following treatment. This observation was accompanied by increasing levels of anti-OVA IgG over time. rAAV1.OVA.miR142BS-transduced muscle tissues showed higher vector genomes than rAAV1.OVA-treated samples at 12 weeks (Supplemental Figure 2), consistent with immune clearance of transduced muscle fibers and loss of vector genomes. Together, these data suggest that animals treated by rAAV1.OVA vector mounted an immunity to the OVA transgene that can be effectively circumvented by incorporating miR142BS into the *Ova* expression cassette.

$CD8^+$ T cell activation plays a major role in transgene immunogenicity. Adaptive immunity against exogenous transgene expression, especially transgenes that are secreted into the circulation, is established by both cellular and humoral immune responses (17). We tested various KO mice for differences in OVA expression between rAAV1.OVA and rAAV1.OVA.miR142BS treatments to determine the contributing components in miR142BS-mediated immune response evasion. Previously, TLR9 has been shown to mediate innate immune responses to AAV vectors (37). To eliminate the role of innate immunity via transgene detargeting, MyD88-KO mice, which lack functional TLR9 signaling, were injected with rAAV1.OVA or rAAV1.OVA.miR142BS vectors (Figure 3A). Mice treated with the latter showed significantly higher levels of OVA compared with those of the rAAV1.OVA injection group, suggesting that TLR9/MyD88 innate immunity is dispensable for enhanced OVA expression by miR-142–mediated detargeting. Further, we injected Rag1-KO mice, which lack mature T and B cells, with rAAV1.OVA or rAAV1.OVA.miR142BS vectors to determine whether miR-142–mediated detargeting affects OVA expression through the modulation of cellular or humoral immunity. Both treatment groups showed similar levels of OVA expression (Figure 3A), suggesting that the enhanced OVA expression in wild-type mice treated with the rAAV miR142BSs is a direct consequence of an attenuated B and/or T cell response. To determine the extent of influence by either the cytotoxic $CD8^+$ T cell response or the B cell humoral response in modulating adaptive immunity against exogenous transgene expression, we compared rAAV1.OVA and rAAV1.OVA.miR142BS vectors in β_2m-KO mice (38) or in μMT mice (39). Interestingly, although the miR142BS element conferred no increase in OVA expression in β_2m-KO mice, we observed significantly higher OVA expression levels in μMT mice treated with rAAV1.OVA.miR142BS compared with those of the rAAV1.OVA-treated group (Figure 3A). This indicated that the loss of OVA expression is primarily driven by an OVA-specific T cell response, which is blunted by the incorporation of miR142BS sequences. In contrast, when

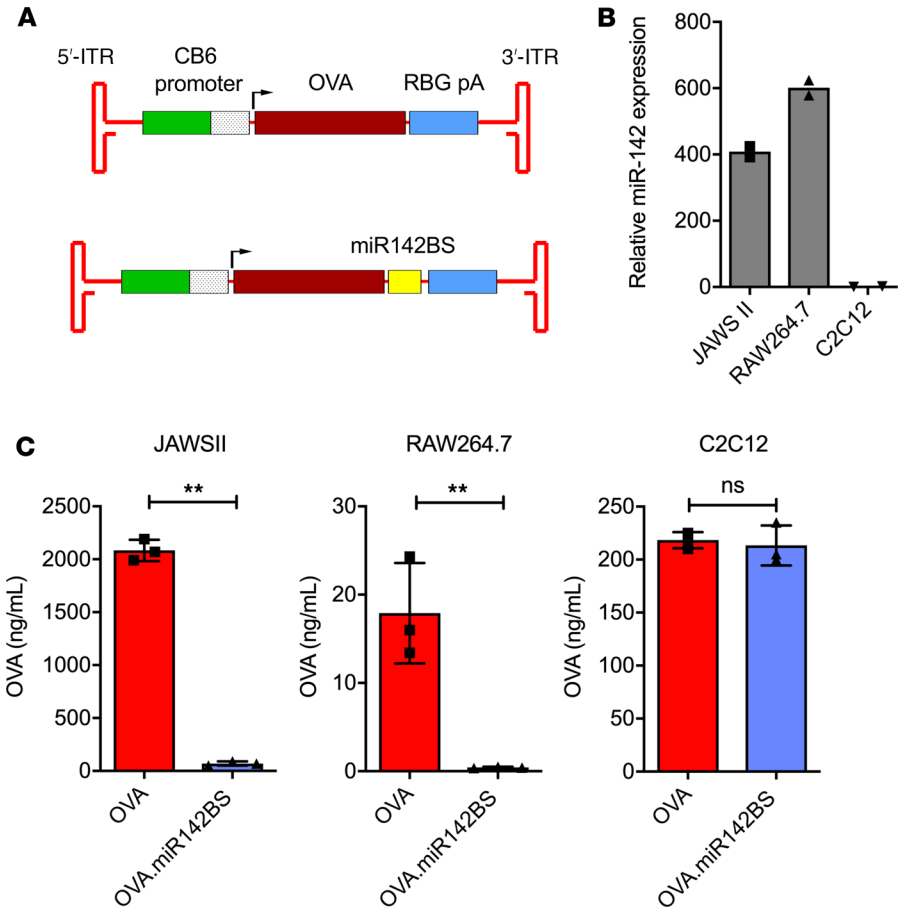

Figure 1. Incorporating miR142BSs into rAAV1 expression cassettes decreases transgene expression in APCs. (**A**) Schematics of rAAV OVA expression vectors. ITRs, inverted terminal repeats; CB, CMV enhancer/chicken β-actin promoter; pA, polyA. (**B**) Endogenous miR-142-3p mRNA expression levels in cultured JAWS II (DCs), RAW264.7 (macrophages), or C2C12 (myoblasts) cells as quantified by reverse transcription quantitative PCR (RT-qPCR) (n = 2). (**C**) JAWS II, RAW264.7, or C2C12 cells were transfected with OVA or OVA.miR142BS plasmids. Seventy-two hours after transfection, supernatants were collected for OVA quantification by ELISA. Bar graphs represent mean ± SD (n = 3). $^{**}P < 0.01$, unpaired t test.

OVA is detargeted from APCs in mice with a mature T cell deficiency, further circumvention of immunity is not observed. This conclusion is further supported by the lack of a significant difference in serum anti-OVA IgG1 between OVA- and OVA.miR142BS-treated β_2m-KO mice (Supplemental Figure 3A). These data support the notion that circumventing adaptive immunity is sufficient for sustained transgene expression.

To corroborate the activation of OVA-specific $CD8^+$ T cells in treated, normal mice, we performed MHC tetramer staining. For this purpose, the tetramer containing 4 H-2Kb MHC class I molecules was bound to the OVA peptide (SIINFEKL) and conjugated with phycoerythrin (PE). We found that 2 weeks after rAAV delivery, the number of OVA-specific $CD8^+$ T cells was significantly lower (>4-fold) in splenocytes isolated from rAAV1.OVA.miR142BS-treated mice than that of the rAAV1.OVA group (Figure 3B). Taken together, these results suggest that reducing transgene expression in APCs sufficiently suppresses the CTL response, and consequently, a muting of the B cell–driven antibody response to the transgene product.

miR142BS detargeting downregulates costimulatory signals in DCs and production of inflammatory cytokines. To study antigen presentation and the associated activation of APCs that is triggered by rAAV1.OVA transduction, we quantified the costimulatory factors expressed in and secreted by DCs. TNF-α is a major proinflammatory cytokine and is involved in both innate and adaptive immune responses (40, 41). TNF-α is produced by DCs and other immune cells and can upregulate CD80/86 costimulatory molecules on DCs (41). Specifically, CD86 (B7-2) interacts with CD28 and is necessary for T cell activation and survival (42). Mice treated with rAAV1.OVA showed a 10-fold increase in circulating TNF-α over rAAV1.OVA.miR142BS- and PBS-treated groups (Figure 3C). Next, we isolated and cultured splenocytes from mice treated with

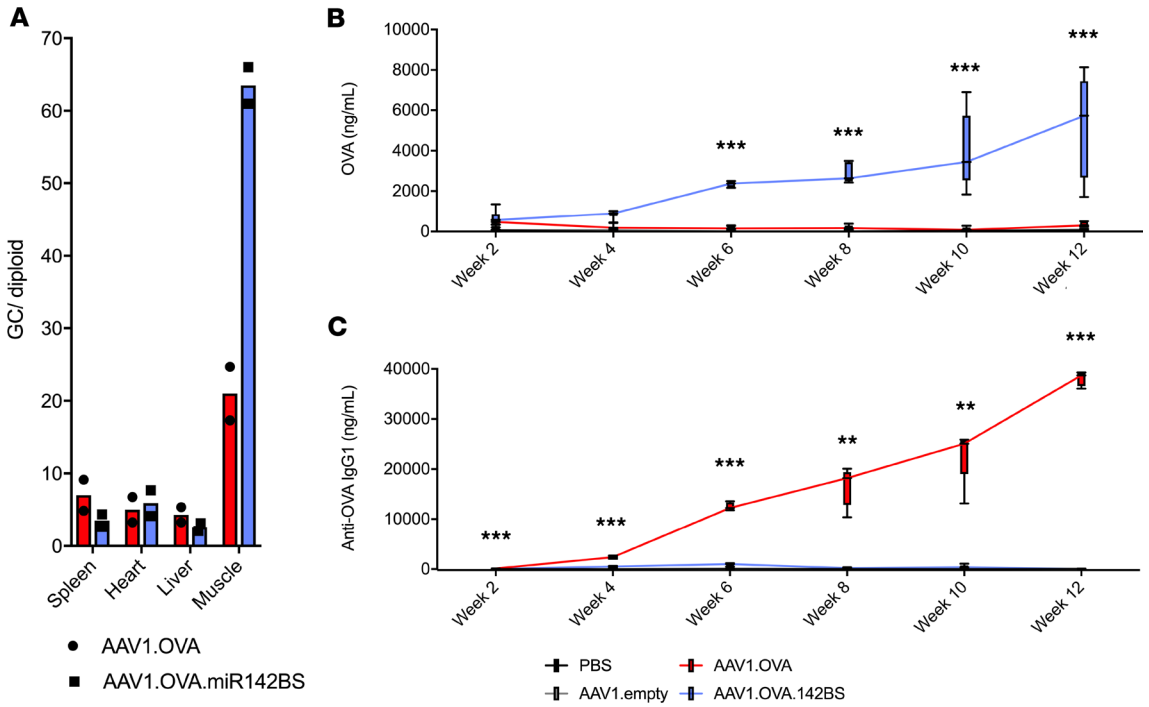

Figure 2. Incorporating miR142BSs sustains OVA expression in vivo. AAV1 injections were carried out on day 0 followed by sera collection every 2 weeks for a 12-week period. (**A**) qPCR detection of rAAV vector genome copies (GCs) in spleen, heart, liver, and injected skeletal muscle (n = 2). (**B** and **C**) ELISA quantification of circulating OVA expression (**B**) and anti-OVA IgG1 (**C**) of mice i.m. injected with rAAV1.OVA or rAAV1.OVA.miR142BS vectors (1×10^{11} GCs/mouse, n = 10). Sera were collected throughout a 12-week period. Box plots with whiskers represent mean ± SD and maximum and minimum values (n = 5). $^{**}P < 0.01$, $^{***}P < 0.001$, ANOVA with Tukey's post hoc test.

PBS, rAAV1.OVA, rAAV1.OVA.miR142BS, or empty AAV1 vector at 4 weeks and 12 weeks after injection. Upon OVA stimulation, rAAV1.OVA splenocytes harvested at 12 weeks secreted high amounts of IFN-γ and TNF-α, demonstrating an anamnestic response to the antigen. In contrast, this response was attenuated in rAAV1.OVA.miR142BS splenocytes (Figure 3, D and E). It is worth noting that the levels of IFN-γ and TNF-α secreted by rAAV1.OVA.miR142BS splenocytes are comparable to those secreted by PBS and empty AAV1 vector splenocytes. This pattern was consistent in splenocytes harvested at 4 weeks (Supplemental Figure 3, B and C), although the reduction in TNF-α levels for rAAV1.OVA.miR142BS splenocytes was not as pronounced as those observed by week 12. In JAWS II cells, OVA-stimulated TNF-α levels were similarly reduced when the miR142BS element was incorporated into the OVA transgene cassette. As expected, levels of TNF-α were unaffected in C2C12s (Supplemental Figure 3, D and E).

Splenocytes positive for CD11c (a marker for myeloid cells, including DCs) were isolated 4 or 12 weeks after rAAV delivery and analyzed for CD86 positivity, a costimulatory marker associated with T cell activation, by flow cytometry. The percentage of $CD86^+$ splenocyte–derived DCs from rAAV1.OVA.miR142BS-treated mice was significantly reduced compared with that of rAAV1.OVA-treated mice at both time points (Figure 3F). The rAAV1 empty capsid group showed comparable levels of $CD11c/CD86^+$ splenocytes to PBS control levels. The difference between OVA- and OVA.miR142BS-treated mice was especially remarkable toward later time points (Figure 3F and Supplemental Figure 4A). This result coincides with significantly reduced TNF-α levels in spleens of rAAV1.OVA.miR142BS-treated mice (Figure 3G and Supplemental Figure 4B).

miR142BS detargeting persistently downregulates transgene immunity upon redosing and further boosts OVA levels. Having established that incorporation of miR142BS suppresses adaptive immunity against the transgene with a single dose of vector, we tested whether it is also effective against repeated vector administration. Adult C57BL/6 mice were i.m. injected with rAAV1.OVA or rAAV1.OVA.miR142BS. Four weeks after the initial injection, a second round of i.m. injections with vector transgenes now packaged in AAV8 capsids (rAAV8.OVA or rAAV8.OVA.miR142BS) was performed (Figure 4, A and B). The AAV8 capsid is serologically distinct from AAV1 (43) and was used to package vector cassettes for redosing to eliminate any capsid-specific immune responses that might confound results. OVA and anti-OVA antibody lev-

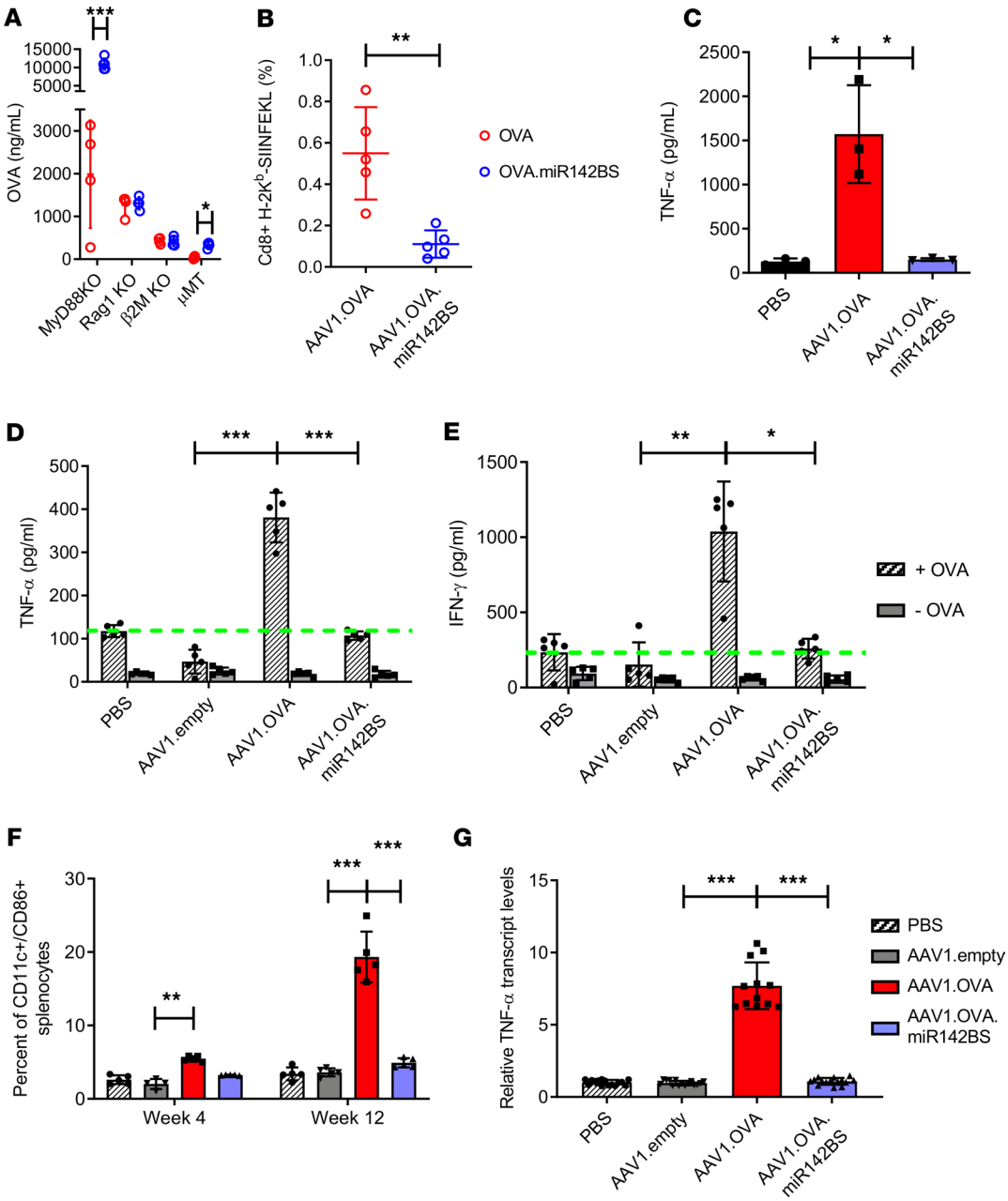

Figure 3. Incorporating miR142BS into the rAAV1.OVA transgene vector results in a decreased OVA-specific T cell response. (**A**) rAAV1.OVA or rAAV1.OVA.miR142BS vectors (1×10^{11} GCs/mouse) were delivered i.m. to MyD88-KO mice, Rag1-KO mice, CD8$^+$ cytolytic T cell–deficient β_2-microglobulin–KO (β_2m-KO) mice and B cell–deficient (μMT) mice. Four weeks after administration, serum OVA levels were measured by ELISA (mean ± SD, $n = 4$). *P* values were determined by unpaired *t* test. (**B**) OVA-specific CD8$^+$ T cells isolated from spleens of vector-injected C57BL/6 mice were stained with anti-CD8a/H-2Kb SIINFEKL tetramer and analyzed by flow cytometry ($n = 4$). *P* values were determined by unpaired *t* test. (**C**) Quantification of serum TNF-α levels by ELISA (mean ± SD, $n = 5$). *P* values were determined by ANOVA with Tukey's post hoc test. (**D** and **E**) Assessment of IFN-γ and TNF-α response to OVA protein (+OVA, 5 μg/mL) by splenocytes isolated from mice 12 weeks after vector injection. Dashed green lines indicate baseline activation values. Three days after treatment, supernatants were collected and quantitated by ELISA (mean ± SD, $n = 5$). *P* values were determined by ANOVA with Tukey's post hoc test. -OVA, mock treatment. (**F**) C57BL/6 male mice, 6 weeks old, were injected i.m. with PBS, rAAV1.OVA, rAAV1.OVA.miR142BS, or AAV1 empty vector (1×10^{11} GCs/mouse). Quantification of CD11c$^+$/CD86$^+$ splenocytes harvested 4 or 12 weeks after vector administration by flow cytometry. Bar graphs represent mean ± SD ($n = 5$). *P* values derived from ANOVA with Holm-Šídák's post hoc test. (**G**) Quantitation of TNF-α mRNA levels in whole spleens by RT-qPCR (mean ± SD, $n = 5$). *P* values were determined by ANOVA with Dunnett's post hoc test. $^*P < 0.05$, $^{**}P < 0.01$, $^{***}P < 0.001$.

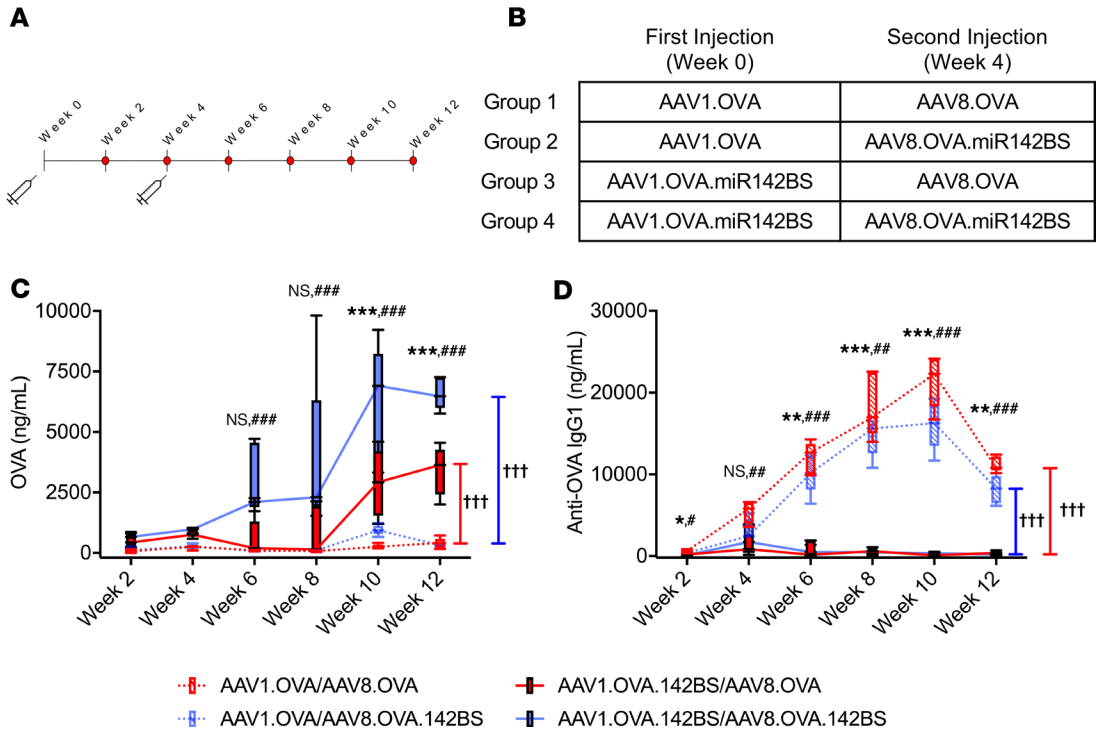

Figure 4. miR142BS-mediated detargeting permits redosing and boosts transgene levels. Timeline for the AAV-redosing experiment (**A**) and the description of the rAAV serotype and OVA transgene specific for each injection (**B**). C57BL/6 male mice, 6 weeks old, were injected i.m. with either rAAV1.OVA or rAAV1.OVA.142BS (1×10^{11} GCs/mouse). The same mice were then redosed with either rAAV8.OVA or rAAV8.OVA.142BS (1×10^{11} GCs/mouse) i.m. 4 weeks after the first injection ($n = 5$). (**C** and **D**) ELISA quantification of circulating OVA expression (**C**) and anti-OVA IgG (**D**) in vector-injected mice. Sera were collected throughout a 12-week period. Box plots with whiskers correspond to mean ± SD and maximum and minimum values. *P* values were determined by ANOVA with Tukey's post hoc test for pairwise comparison. Asterisks (*) denote test of significance between injection groups 1 and 3, and hashes (#) denote test of significance between injection groups 2 and 4. *P* values for longitudinal comparisons were determined by repeated measures with 2-way ANOVA. Daggers (†) denote test of significance. $^{*,\#}P < 0.05$, $^{**,\#\#}P < 0.01$, $^{***,\#\#\#,\dagger\dagger\dagger}P < 0.001$.

els in serum were then measured over the course of 12 weeks. Mice initially injected with rAAV1.OVA.miR142BS vectors followed by rAAV8.OVA with or without miR142BS generated enhanced and sustained levels of OVA with negligible levels of anti-OVA IgG1 in the circulation (Figure 4, C and D). Notably, OVA expression was boosted further when OVA.miR142BS was readministered with the second injection only when OVA.miR142BS was administered with the first injection (Figure 4C, solid blue tracks). In contrast, mice that were first dosed with rAAV1.OVA showed near-baseline levels of serum OVA and high anti-OVA IgG1 levels, irrespective of whether the second injected vector transgene carried the miR142BS element.

The overall reduction of transgene expression is primarily due to the clearance of transduced cells by a CD8⁺ T cell response. We next assessed the functionality of the OVA-specific CD8⁺ cells in the spleens of animals receiving rAAV1.OVA with or without miR142BS sequences by an in vivo CTL assay (30). This analysis quantifies functional CTLs of adoptively transferred and CFSE-labeled target cells (Figure 5A and ref. 44). Seventeen days after rAAV1 delivery, rAAV1.OVA-treated mice displayed a 76% clearance of target cells, corresponding to 20 ng/mL of serum OVA, whereas rAAV1.OVA.miR142BS-injected mice had a significant reduction in the clearance of OVA-specific target cells (approximately 20%), with an increase in OVA serum levels (170 ng/mL) (Figure 5, B and C).

To further characterize the reduction of transgene-specific T cell response by miR142BS, we analyzed the histopathology of injected muscle tissues, followed by immunohistochemical staining for CD8⁺ cells 2 weeks after rAAV1.OVA or rAAV1.OVA.miR142BS treatment. H&E staining of the AAV1.OVA-injected TA muscles showed severe cellular infiltration (Figure 5, D and E). Immunohistochemical staining indicated that some of these infiltrates were CD8⁺. In contrast, injected muscles receiving rAAV1.OVA.miR142BS had little infiltration of immune cells, and no CD8⁺ cells were detected (Figure 5D). This finding indicates that inclusion of miR142BS elements in the OVA transgene reduces clearance of transduced muscle fibers because of a reduced infiltration of CD8⁺ T cells. This outcome in part supports Figure 2B and Supplemen-

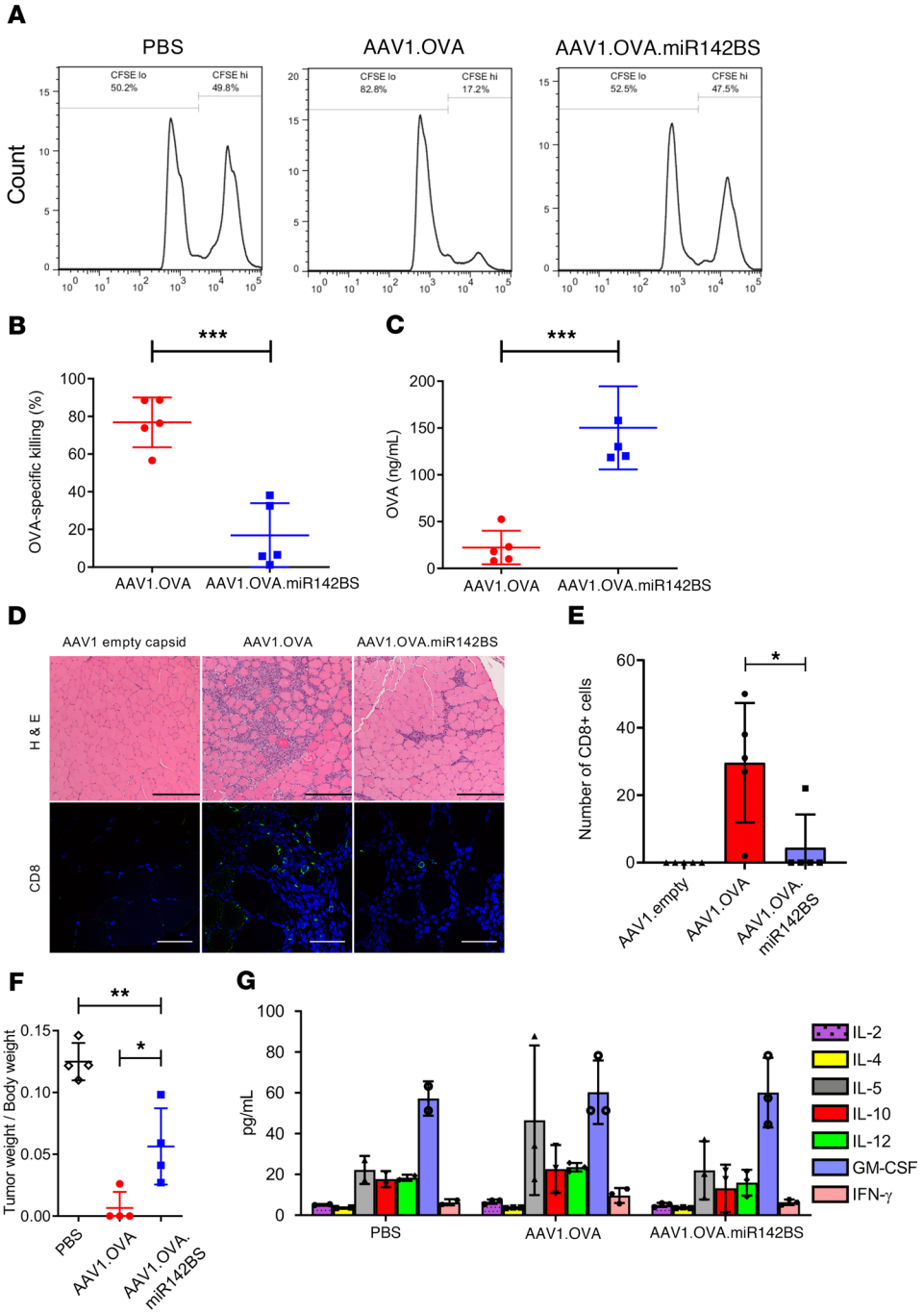

Figure 5. Transgene detargeting of DCs with miR142BS reduces CD8⁺ infiltrates and OVA-specific tissue clearance. (**A** and **B**) In vivo CTL assay of vector-treated animals. (**A**) C57BL/6 male mice, 6 weeks old, were i.m. injected with PBS, rAAV1.OVA, or rAAV1.OVA.miR142BS (1×10^{11} GCs/mouse). Seventeen days after injection, target cells from the spleens of the same strain of treatment-naive mice were either labeled with a high concentration of CFSE ($CFSE^{hi}$, 5 μM) and pulsed with SIINFEKL peptide (OT-1, 1 μg/mL) or labeled with a low concentration of CFSE ($CFSE^{lo}$, 0.5 μM) and not pulsed. (**B**) Populations of target cells were mixed (1:1) and cotransferred intravenously (4×10^7 cells) to PBS- or AAV1-treated mice. Six hours later, splenocytes were isolated and analyzed by flow cytometry to determine the percentage of remaining target cells. Bar graphs represent mean ± SD ($n = 5$). ***$P < 0.001$, unpaired t test. (**C**) Serum OVA levels in AAV1.OVA- or AAV1.OVA.miR142BS-treated mice were measured by ELISA (mean ± SD, $n = 5$). ***$P < 0.001$, unpaired t test. (**D**) C57BL/6 male mice, 6 weeks old, were i.m. injected with rAAV1.OVA, rAAV1.OVA.miR142BS, or AAV1 empty vector (1×10^{11} GCs/mouse, $n = 5$). Two weeks after injection, muscles were harvested for H&E (left, original magnification: ×10) and CD8 staining (right; green, anti-CD8; blue, DAPI; original magnification: ×40). Scale bars: 250 μm (H&E images), 50 μm (fluorescence images). (**E**) Quantitation of $CD8^+$ T cells counted in 4 fields at original magnification of ×20. *$P < 0.05$, unpaired t test ($n = 5$). (**F**) AAV1.OVA.miR142BS-treated C57BL/6 mice show reduced tumor killing after E.G7-OVA lymphoma cell inoculation. C57BL/6 male mice, 6 weeks old, were injected i.m. with AAV1.OVA or AAV1.OVA.miR142BS (1×10^{11} GCs/mouse). Two weeks after injection, the OVA-expressing E.G7 cells were subcutaneously inoculated (2×10^6 cells/mouse, $n = 4$). Ten days after inoculation, tumors were harvested and weighed. *$P < 0.05$, **$P < 0.01$; 1-way ANOVA followed by Tukey's test. (**G**) Serum levels of Th1 and Th2 cytokines in mice treated with AAV1 vectors. C57BL/6 male mice, 6 weeks old, were i.m. injected with PBS, rAAV1.OVA, or rAAV1.OVA.miR142BS (1×10^{11} GCs/mouse). Two weeks later, serum levels of the cytokines IFN-γ, IL-2, IL-4, IL-5, IL-10, IL-12, and GM-CSF were determined by multiple Bio-Plex analysis. Bar graphs represent mean ± SD ($n = 3$).

tal Figure 2 data, where vector genome copies were significantly diminished (3-fold) in muscles treated with rAAV1.OVA as compared with those that received rAAV1.OVA.miR142BS.

We next aimed to corroborate the functionality of OVA-specific CTLs generated by rAAV1.OVA with or without an miR142BS sequence. Wild-type C57BL/6 mice were subcutaneously inoculated with a mouse T cell lymphoma cell line expressing OVA protein (E.G7-OVA). Two weeks following rAAV injection, E.G7-OVAs presented with OT-1 by MHC class I molecules (data not shown). Ten days after inoculation, tumors developed in PBS- and rAAV1.OVA.miR142BS-treated mice but not in rAAV1.OVA-treated mice (Figure 5F). These data indicate that the rAAV1.OVA-treated mice generate a robust OVA-specific CTL response that completely inhibits tumor growth, while rAAV1.OVA.miR142BS-treated mice exhibit a significantly weaker OVA-specific T cell response and are unable to sufficiently suppress tumor growth. Although on average, the tumor/body weight ratios of the rAAV1.OVA.miR142BS-treated mice did not reach those of PBS-treated mice, we show that after 10 days of treatment, tissue clearance is clearly and significantly attenuated because of transgene-specific CTL (Figure 5F).

Last, we gauged the contribution of the humoral response that is elicited by OVA when detargeted from APCs. Humoral immunity is initiated by the activation of Th cells. During the proliferation and differentiation of these $CD4^+$ T cells into Th1 and Th2 populations, Th1 and Th2 cytokines are secreted. To profile the Th response as a consequence of rAAV1.OVA or rAAV1.OVA.miR142BS treatment, we assayed the change in a few selected cytokines (IFN-γ, IL-2, IL-4, IL-5, IL-10, IL-12, and GM-CSF) in the serum. Strikingly, we saw no significant difference between PBS, rAAV1.OVA, and rAAV1.OVA.miR142BS treatment groups in cytokine levels (Figure 5G). This finding suggests that overcoming cell-mediated immunity is sufficient to overcome adaptive immunity against a secreted foreign transgene, allowing stable expression of a therapeutic gene product in circulation.

Discussion

Skeletal muscle has been shown to be an important target tissue for rAAV-mediated gene therapy of muscle diseases, gene augmentation, and metabolic disorders (45–48). Recent demonstration of host immunity against rAAV1-encoded transgene products delivered i.m. in monkeys (6, 7) has raised concerns that undesirable rAAV transduction of APCs can result in transgene expression, processing, and presentation by DCs. This outcome results in the stimulation of a CTL response and the destruction of transduced cells — counterproductive to transgene expression and therapy. Studies have shown that several rAAVs, including rAAV1, have the capacity to transduce DCs and initiate an immune response to transgene products (49, 50). This phenomenon occurs despite the use of tissue-specific promoters to drive transgene expression (17, 18). Therefore, developing strategies to detarget transgene expression from DCs is of particular relevance for rAAV-mediated gene transfer modalities.

Although several studies have demonstrated that miR-142 target sites can successfully decrease an immune response mounted against an exogenously delivered transgene (21, 22, 31), there is intriguing evidence that this action is context dependent (18). In this study, we show that the detargeting of OVA in APCs results in the blunting of CTL activation (Figure 3A). It is conceivable that other factors, like strain-related differences in AAV transduction, contribute to varied immune responses. For example, we observed a nearly 60% decrease in OVA expression in β_2m-KO mice compared with Rag1-KO mice. Although rAAV transduction efficiency in different mouse lines may be the cause for the variance in observed OVA levels, it is uncertain whether this is imparted by B cell activation, which remains intact in β_2m-KO mice, although our data seem to contradict this explanation because anti-OVA IgG was drastically reduced and remained low in animals treated with OVA.miR142BS for the duration of our experimental window (Figure 2C). In addition, humoral response–related Th1 and Th2 cytokine levels were not significantly different in either rAAV1.OVA or rAAV1.OVA.miR142BS treatment groups from the control treatment group (Figure 5G).

The delivery of exogenously expressed transcripts carrying miR142BSs by rAAV1 also did not result in any clear effect on overall T cell activation that was reflected in serum cytokine levels (Figure 5G). This is a substantial and unexpected finding because miR142 is expressed in all cell types of the hematopoietic lineage, and overexpression of miR142 has been shown by others to reduce the uptake and processing of soluble OVA in primary human macrophages and DCs (51). Unfortunately, exploration into whether reducing miR-142 activity in APCs could impair overall T cell function (e.g., via an unknown anergy mechanism) is currently limited. Such studies could help to further understand how the humoral response is overcome when high levels of circulating OVA are achieved following APC detargeting.

Although terminally differentiated tissues, such as liver and muscle, are preferred targets for long-term, in vivo transduction of rAAV, episomal and nonreplicating rAAV genomes may gradually become lost over time, as a result of host cell turnover. Thus, the development of effective therapeutic strategies for diseases may require repeated administration of vectors. Our redosing studies clearly demonstrate that injection of rAAV1.OVA.miR142BS successfully suppressed cell-mediated immune response, even under circumstances that may require readministration of the therapy (Figure 4, C and D). Furthermore, the effectiveness of miR142BS-mediated suppression of transgene immunity is reliant on miR-142 expression in APCs within tissues of interest. Other miRNA-binding sites could also serve to detarget from problematic tissues or cell types. For example, it has been demonstrated that incorporation of miR122-binding sites effectively detargets transgene expression from the liver. Future combinatorial miRBS designs may further enhance this effective platform for controlling transgene expression.

It is well accepted that cross-presentation is important for $CD8^+$ T cell responses against secreted proteins (52). However, our findings demonstrate that the suppression of antigen expression in APCs was sufficient to reduce the $CD8^+$ T cell response and prevent unwanted antibody responses against the transgene product. Importantly, we demonstrate that miR142BS was sufficient for attenuating the clearance of transduced muscles as well as E.G7-OVA xenographs. Unfortunately, our results do not fully resolve the context dependency observed for miR-mediated detargeting in the *Sgca*$^{-/-}$ model, as shown by Boisgerault et al. (18). As cited in the aforementioned study, it is plausible that in the *Sgca*$^{-/-}$ model, the inflamed dystrophic myofibers may increase indirect antigen presentation. In addition, whether miR142BS elements can also overturn self-epitope immunity is not known. For example, the mini-dystrophin transgene has been shown to prime a dystrophin-specific T cell response, becoming destructive to revertant fibers, which are a small percentage of functional myofibers that undergo alternative splicing to generate natively expressed functional dystrophin (12). We demonstrate here that OVA levels were sustained up to 12 weeks after injection (Figure 2) and OVA-specific IgGs were concomitantly low. Our findings may offer a promising solution to overcoming scenarios where immunity to natively expressed proteins can be counterproductive to therapy. Nonetheless, we provide additional lines of evidence that, at least for secreted factors where the muscle serves as an ectopic transgene biofactory, immune stimulation and tissue clearance can be circumvented via miR-142–mediated regulation. Delivery of tetanus toxoid, CMV antigen, or a clinically relevant secreted agent, such as α-1 antitrypsin, factor IX, or neutralizing antibodies, would help toward understanding the context dependency for miR-mediated detargeting and related limitations of the approach observed by others. Ultimately, our findings reinforce the promise for rAAV-mediated muscle gene transfer as a therapeutic and prophylactic modality for treating and preventing human diseases.

Methods

Vector plasmid construction and rAAV production. Full-length *OVA* cDNA was inserted in the *cis*-plasmid of the rAAV expression cassette between the CB promoter and rabbit β-globin (*RBG*) polyA signal to generate pAAV.CB.*OVA*. For pAAV.CB.*OVA*.miRNA142BS constructs, 2 copies of synthesized miR142BS sequences (5′-TCCATAAAGTAGGAAACACTACA-3′) were inserted between the *OVA* cDNA and *RBG* polyA signal. All expression cassettes were verified by Sanger sequencing. rAAV1 and rAAV8 vectors were produced by the Viral Vector Core at the University of Massachusetts Medical School as previously described (53).

Mice. C57BL/6, B6.129P2(SJL)-Myd88$^{tm1.1}$Defr/J (myd88-null), B6.129S2-Igh-6tm1Cgn (μMT), B6.129S7-Rag1tm1Mom (Rag1-KO), and B6.129P2-B2mtm1Unc (β_2m-KO) mice were purchased from The Jackson Laboratory and maintained at the University of Massachusetts Medical School. Mice were housed under specific pathogen–free conditions. Male mice, 6–8 weeks old, were injected via TA muscles with 1.0×10^{11} GCs of rAAV1 diluted in sterile PBS. Blood samples were collected via facial vein by using an animal lancet (Goldenrod) and BD Microtainer tubes with serum separator additive (Becton Dickinson and Company).

ELISA. Serum levels of OVA and anti-OVA IgG were determined by ELISA. Briefly, 96-well Nunc Maxisorp Immunoplates (Thermo Fisher Scientific) were coated with 2 μg/mL of rabbit anti-OVA polyclonal antibodies (AB1225, MilliporeSigma) or OVA protein (MilliporeSigma) in 100 μL coating buffer (KPL) per well. After overnight incubation at 4°C, the plates were washed with 0.05% Tween-20 in PBS, followed by incubation with blocking buffer (KPL) for 2 hours at room temperature. For OVA detection, the samples were diluted 100-fold with ELISA diluent (KPL), and OVA protein standards (Bioworld) were 2-fold serially diluted with 1% normal mouse serum starting from 50 ng/mL. Then 100 μL of sample or standard was added to plates and incubated for 1 hour at room temperature. After washing 4 times, peroxidase-conjugated rabbit

anti-OVA polyclonal antibody (200-4333-0100, Rockland Immunochemicals) (1:5000 diluted) was added and incubated for 1 hour at room temperature. For anti-OVA IgG1 detection, samples were diluted 1:200, and the mouse anti-OVA IgG1 (sc-80589, Santa Cruz Biotechnology) was used as the standard. After a 1-hour incubation in OVA-coated plates, wells were washed, HRP-conjugated goat anti-mouse IgG1 (sc-2060, Santa Cruz Biotechnology) was added, and plates were incubated for another hour at room temperature. Plates were then washed 4 times and incubated with 100 μL of ABTS HRP Substrate (KPL). Optical density at 410 nm was measured using a Synergy HT microplate reader (BioTek). Standard curves for OVA and IgG1 were generated by using the 4-parameter logistic regression with Gen5 software (BioTek).

In vitro screening for OVA constructs. OVA expression plasmids with or without the miR142BS element were transfected into mouse myoblast C2C12 cells (ATCC, CRL-1772) and the macrophage cell line RAW264.7 (ATCC, TIB-71) using jetPRIME transfection reagents (Polyplus-transfection SA) according to the manufacturer's instructions. C2C12 and RAW264.7 cells were cultured in Dulbecco's modified Eagle medium (Hyclone, SH30022) with 10% fetal bovine serum (FBS, Hyclone, SH30071) and 1% penicillin/streptomycin (Hyclone, SV30010). Mouse dendritic JAWS II cells (ATCC, CRL-11904) were cultured in α minimum essential medium (MilliporeSigma, M8042) with ribonucleosides, deoxyribonucleosides, 4 mM L-glutamine, 1 mM sodium pyruvate, and 20% FBS with 5 ng/mL murine GM-CSF. JAWS II were transfected by Nucleofection. Briefly, 2.0×10^6 cells were collected and resuspended in 100 μL Nucleofector Solution (Lonza, V4XP-4024) at room temperature. Plasmids were then added, the mixture was transferred into Nucleocuvette Vessels, and the program (P4 HF) was selected for immature mouse DCs (Lonza). Then 2 mL of medium was added, and cells were split into a 24-well plate (500 μL/well) (Corning, CLS3527). Three days after transfection, supernatants were collected for OVA ELISA.

In vivo CTL assay. We injected 6-week-old C57BL/6 male mice with PBS, rAAV1.OVA, or rAAV1.OVA.miR142BS into the TA. Seventeen days after injection, splenocytes from naive C57BL/6 mice were isolated by mashing spleens through a 70-μm Cell Strainer (BD Biosciences, 352350). After lysis of red blood cells, the suspensions were centrifuged at 200 *g* for 3 minutes. The remaining splenocyte cell pellets were washed twice with RPMI 1640 medium (Thermo Fisher Scientific, catalog 22400089). Splenocytes were then suspended in sterile PBS and labeled with either high concentration of CFSE ($CFSE^{hi}$, 5 μM) and pulsed with SIINFEKL peptide (OT-1, 1 μg/mL) or labeled with a low concentration of CFSE ($CFSE^{lo}$, 0.5 μM) and not pulsed. The populations of target cells were mixed (1:1) and cotransferred intravenously (4×10^7 cells) to PBS- or rAAV1-treated mice. Six hours later, splenocytes were isolated and analyzed by flow cytometry to determine the percentage of remaining target cells. The specific killing activity was calculated with the following formulas: The percentage of specific killing = (1 − ratio from control, unprimed recipient/ratio from primed recipient) × 100; the ratio = percentage of unpulsed $CFSE^{lo}$ cells/percentage of pulsed $CFSE^{hi}$ cells.

Flow cytometry. Cells were suspended in 100 μL PBS with 1% FBS and incubated with anti-CD16/32 (2.4G2) mAb (BD Biosciences, catalog 553141) for 15 minutes at 4°C. After blocking, the corresponding antibodies were added for 30 minutes at 4°C. The PE–anti-CD11c (HL3) mAb was purchased from BD Biosciences (catalog 553802) and the APC–anti-CD86 (GL-1) mAb was purchased from BioLegend (catalog 105011). For tetramer staining, mouse blood samples were collected into BD Microtainer tubes with dipotassium EDTA. The FITC rat anti-mouse CD8a mAb (BioLegend) and iTAg MHC Tetramer H-2Kb SIINFEKL-PE (T03000, MBL) were added to samples and incubated for 30 minutes at 4°C. Samples were then processed according to the manufacturers' instructions. The flow cytometric analysis was performed on Guava easyCyte 8HT (MilliporeSigma). Data were analyzed using FlowJo (Tree Star).

Tumor growth model. Male C57BL/6 mice, 8 weeks old, were subcutaneously inoculated on the flanks with 2×10^6 E.G7-OVA cells (ATCC, CRL-2113). Tumor volume was calculated by the following formula: tumor volume = 0.4 × length (mm) × width (mm). When tumor volume reached 500 mm^3, the mice were euthanized. Tumor tissues were harvested and weighed.

qPCR and RT-qPCR. Mouse tissue DNA was isolated using the QIAamp genomic DNA kit (QIAGEN) following the manufacturer's instructions. Detection and quantification of vector genomes in extracted DNA were performed by real-time qPCR as described previously (54, 55). Total RNA was isolated from mouse tissues or cells using Trizol (Life Technologies). RT real-time qPCR was performed using the ViiA 7 real-time PCR system (Life Technologies) to detect TNF-α and miR-142-3p expression levels. The reagents and primers for miRNA quantification were purchased from Exiqon (now a QIAGEN company). All other reagents, primers, and probes were purchased from Life Technologies.

Immunohistochemistry. Mouse tissues were fixed in 10% formalin buffer (Fisher Scientific, catalog SF100-20) overnight and embedded in paraffin. Sections (8 μm thick) were stained with H&E. Images were acquired on a Leica DM5500 B microscope using a ×10 objective.

For CD8a staining, muscle sections were processed at Dana-Farber/Harvard Cancer Center Specialized Histopathology Services and Beth Israel Deaconess Medical Center histology core facilities. Sections were stained for CD8 (1:500, D4W2Z, Cell Signaling Technology). Antibodies were tagged with Alexa Fluor 488 Tyramide (B40957, Thermo Fisher Scientific). All immunohistochemistry was performed on the Leica Bond automated staining platform using the Leica Biosystems Refine Detection Kit with citrate antigen retrieval. Images were acquired on a Zeiss LSM710 laser scanning confocal microscope using a ×40 oil-immersion objective.

Statistics. All data are shown as mean ± SD. Unpaired Student's *t* tests (2-tailed) and 2-way ANOVA, with or without post hoc testing, were calculated using GraphPad Prism 8. Differences were considered significant when *P* values were less than 0.05.

Study approval. All animal procedures were approved by the Institutional Animal Care and Use Committee of the University of Massachusetts Medical School. Experiments were conducted in accordance with relevant guidelines and regulations.

Author contributions

YX, MM, SL, WQ, GX, LL, JL, SKW, AJL, YKC, CW, MAN, and DW performed the experiments. QS produced all the AAV vectors. GMC, LY, YW, PWLT, RCD, CM, and GG supervised the study. MF, RCD, and GG applied for the grants. YX, MM, SL, WQ, GX, LL, JL, AJL, SKW, YKC, CW, SPF, DW, QS, MAN, GMC, MF, LY, YW, RCD, CM, PWLT, and GG discussed the data and contributed to the drafting of the manuscript.

Acknowledgments

This work was supported by grants from the NIH: 1R01NS076991 and UG3 HL147367-01 (to GG), R01DK098252 (to CM), P01AI1002630 (to RCD, MF, and GG), and P01HL131471 (to CM and GG).

Address correspondence to: Christian Mueller, Phillip W.L. Tai, or Guangping Gao, Horae Gene Therapy Center, University of Massachusetts Medical School, 368 Plantation Street, AS6-2049, Worcester, Massachusetts 01605, USA. Phone: 508.856.4358; Email: Chris.Mueller@umassmed.edu (C. Mueller). Phone: 774.455.4559; Email: Phillip.Tai2@umassmed.edu (P.W.L. Tai). Phone: 508.856.3563; Email: Guangping.Gao@umassmed.edu (G. Gao).

1. Wang D, Zhong L, Nahid MA, Gao G. The potential of adeno-associated viral vectors for gene delivery to muscle tissue. *Expert Opin Drug Deliv*. 2014;11(3):345–364.
2. Naldini L. Gene therapy returns to centre stage. *Nature*. 2015;526(7573):351–360.
3. Samulski RJ, Muzyczka N. AAV-mediated gene therapy for research and therapeutic purposes. *Annu Rev Virol*. 2014;1(1):427–451.
4. Daya S, Berns KI. Gene therapy using adeno-associated virus vectors. *Clin Microbiol Rev*. 2008;21(4):583–593.
5. Balazs AB, Chen J, Hong CM, Rao DS, Yang L, Baltimore D. Antibody-based protection against HIV infection by vectored immunoprophylaxis. *Nature*. 2011;481(7379):81–84.
6. Johnson PR, et al. Vector-mediated gene transfer engenders long-lived neutralizing activity and protection against SIV infection in monkeys. *Nat Med*. 2009;15(8):901–906.
7. Fuchs SP, Martinez-Navio JM, Piatak M, Lifson JD, Gao G, Desrosiers RC. AAV-delivered antibody mediates significant protective effects against SIVmac239 challenge in the absence of neutralizing activity. *PLoS Pathog*. 2015;11(8):e1005090.
8. Gardner MR, et al. AAV-expressed eCD4-Ig provides durable protection from multiple SHIV challenges. *Nature*. 2015;519(7541):87–91.
9. de Jong YP, et al. Broadly neutralizing antibodies abrogate established hepatitis C virus infection. *Sci Transl Med*. 2014;6(254):254ra129.
10. Deal C, Balazs AB, Espinosa DA, Zavala F, Baltimore D, Ketner G. Vectored antibody gene delivery protects against Plasmodium falciparum sporozoite challenge in mice. *Proc Natl Acad Sci U S A*. 2014;111(34):12528–12532.
11. Limberis MP, et al. Intranasal antibody gene transfer in mice and ferrets elicits broad protection against pandemic influenza. *Sci Transl Med*. 2013;5(187):187ra72.
12. Mendell JR, et al. Dystrophin immunity in Duchenne's muscular dystrophy. *N Engl J Med*. 2010;363(15):1429–1437.
13. Gao G, et al. Erythropoietin gene therapy leads to autoimmune anemia in macaques. *Blood*. 2004;103(9):3300–3302.
14. Chenuaud P, et al. Autoimmune anemia in macaques following erythropoietin gene therapy. *Blood*. 2004;103(9):3303–3304.
15. Jooss K, Yang Y, Fisher KJ, Wilson JM. Transduction of dendritic cells by DNA viral vectors directs the immune response to transgene products in muscle fibers. *J Virol*. 1998;72(5):4212–4223.
16. Mays LE, Wilson JM. The complex and evolving story of T cell activation to AAV vector-encoded transgene products. *Mol*

Ther. 2011;19(1):16–27.
17. Wang L, Dobrzynski E, Schlachterman A, Cao O, Herzog RW. Systemic protein delivery by muscle-gene transfer is limited by a local immune response. *Blood*. 2005;105(11):4226–4234.
18. Boisgerault F, et al. Prolonged gene expression in muscle is achieved without active immune tolerance using microrRNA 142.3p-regulated rAAV gene transfer. *Hum Gene Ther*. 2013;24(4):393–405.
19. Bartel DP. MicroRNAs: genomics, biogenesis, mechanism, and function. *Cell*. 2004;116(2):281–297.
20. Pasquinelli AE. MicroRNAs and their targets: recognition, regulation and an emerging reciprocal relationship. *Nat Rev Genet*. 2012;13(4):271–282.
21. Brown BD, Venneri MA, Zingale A, Sergi Sergi L, Naldini L. Endogenous microRNA regulation suppresses transgene expression in hematopoietic lineages and enables stable gene transfer. *Nat Med*. 2006;12(5):585–591.
22. Brown BD, et al. A microRNA-regulated lentiviral vector mediates stable correction of hemophilia B mice. *Blood*. 2007;110(13):4144–4152.
23. Xie J, et al. MicroRNA-regulated, systemically delivered rAAV9: a step closer to CNS-restricted transgene expression. *Mol Ther*. 2011;19(3):526–535.
24. Qiao C, et al. Liver-specific microRNA-122 target sequences incorporated in AAV vectors efficiently inhibits transgene expression in the liver. *Gene Ther*. 2011;18(4):403–410.
25. Geisler A, et al. Application of mutated miR-206 target sites enables skeletal muscle-specific silencing of transgene expression of cardiotropic AAV9 vectors. *Mol Ther*. 2013;21(5):924–933.
26. Georgiadis A, et al. AAV-mediated knockdown of peripherin-2 in vivo using miRNA-based hairpins. *Gene Ther*. 2010;17(4):486–493.
27. Turner ML, Schnorfeil FM, Brocker T. MicroRNAs regulate dendritic cell differentiation and function. *J Immunol*. 2011;187(8):3911–3917.
28. Danger R, Braza F, Giral M, Soulillou JP, Brouard S. MicroRNAs, Major players in B cells homeostasis and function. *Front Immunol*. 2014;5:98.
29. Squadrito ML, Etzrodt M, De Palma M, Pittet MJ. MicroRNA-mediated control of macrophages and its implications for cancer. *Trends Immunol*. 2013;34(7):350–359.
30. Chen CZ, Li L, Lodish HF, Bartel DP. MicroRNAs modulate hematopoietic lineage differentiation. *Science*. 2004;303(5654):83–86.
31. Majowicz A, et al. Mir-142-3p target sequences reduce transgene-directed immunogenicity following intramuscular adeno-associated virus 1 vector-mediated gene delivery. *J Gene Med*. 2013;15(6–7):219–232.
32. Xiao W, Berta SC, Lu MM, Moscioni AD, Tazelaar J, Wilson JM. Adeno-associated virus as a vector for liver-directed gene therapy. *J Virol*. 1998;72(12):10222–10226.
33. Alexopoulou AN, Couchman JR, Whiteford JR. The CMV early enhancer/chicken beta actin (CAG) promoter can be used to drive transgene expression during the differentiation of murine embryonic stem cells into vascular progenitors. *BMC Cell Biol*. 2008;9:2.
34. Wang Z, et al. Adeno-associated virus serotype 8 efficiently delivers genes to muscle and heart. *Nat Biotechnol*. 2005;23(3):321–328.
35. Weitzman MD, Thistlethwaite PA. Breaking the barriers to global gene delivery. *Nat Biotechnol*. 2005;23(3):305–306.
36. Calcedo R, et al. Class I-restricted T-cell responses to a polymorphic peptide in a gene therapy clinical trial for α-1-antitrypsin deficiency. *Proc Natl Acad Sci U S A*. 2017;114(7):1655–1659.
37. Zhu J, Huang X, Yang Y. The TLR9-MyD88 pathway is critical for adaptive immune responses to adeno-associated virus gene therapy vectors in mice. *J Clin Invest*. 2009;119(8):2388–2398.
38. Zijlstra M, Bix M, Simister NE, Loring JM, Raulet DH, Jaenisch R. Beta 2-microglobulin deficient mice lack CD4-8$^+$ cytolytic T cells. *Nature*. 1990;344(6268):742–746.
39. Kitamura D, Roes J, Kühn R, Rajewsky K. A B cell-deficient mouse by targeted disruption of the membrane exon of the immunoglobulin mu chain gene. *Nature*. 1991;350(6317):423–426.
40. Pasparakis M, Alexopoulou L, Episkopou V, Kollias G. Immune and inflammatory responses in TNFα-deficient mice: a critical requirement for TNFα in the formation of primary B cell follicles, follicular dendritic cell networks and germinal centers, and in the maturation of the humoral immune response. *J Exp Med*. 1996;184(4):1397–1411.
41. Fujii S, Liu K, Smith C, Bonito AJ, Steinman RM. The linkage of innate to adaptive immunity via maturing dendritic cells in vivo requires CD40 ligation in addition to antigen presentation and CD80/86 costimulation. *J Exp Med*. 2004;199(12):1607–1618.
42. Chen L, Flies DB. Molecular mechanisms of T cell co-stimulation and co-inhibition. *Nat Rev Immunol*. 2013;13(4):227–242.
43. Gao G, et al. Clades of Adeno-associated viruses are widely disseminated in human tissues. *J Virol*. 2004;78(12):6381–6388.
44. Chen J, Wu Q, Yang P, Hsu HC, Mountz JD. Determination of specific CD4 and CD8 T cell epitopes after AAV2- and AAV8-hF.IX gene therapy. *Mol Ther*. 2006;13(2):260–269.
45. Mendell JR, et al. Gene therapy for muscular dystrophy: lessons learned and path forward. *Neurosci Lett*. 2012;527(2):90–99.
46. Ross CJ, et al. Correction of feline lipoprotein lipase deficiency with adeno-associated virus serotype 1-mediated gene transfer of the lipoprotein lipase S447X beneficial mutation. *Hum Gene Ther*. 2006;17(5):487–499.
47. Brantly ML, et al. Sustained transgene expression despite T lymphocyte responses in a clinical trial of rAAV1-AAT gene therapy. *Proc Natl Acad Sci U S A*. 2009;106(38):16363–16368.
48. Wierzbicki AS, Viljoen A. Alipogene tiparvovec: gene therapy for lipoprotein lipase deficiency. *Expert Opin Biol Ther*. 2013;13(1):7–10.
49. Hadaczek P, et al. Transduction of nonhuman primate brain with adeno-associated virus serotype 1: vector trafficking and immune response. *Hum Gene Ther*. 2009;20(3):225–237.
50. Xin KQ, et al. Induction of robust immune responses against human immunodeficiency virus is supported by the inherent tropism of adeno-associated virus type 5 for dendritic cells. *J Virol*. 2006;80(24):11899–11910.
51. Naqvi AR, Fordham JB, Ganesh B, Nares S. miR-24, miR-30b and miR-142-3p interfere with antigen processing and presentation by primary macrophages and dendritic cells. *Sci Rep*. 2016;6:32925.
52. Carbone FR, Bevan MJ. Class I-restricted processing and presentation of exogenous cell-associated antigen in vivo. *J Exp Med*. 1990;171(2):377–387.
53. Mueller C, Ratner D, Zhong L, Esteves-Sena M, Gao G. Production and discovery of novel recombinant adeno-associated viral vectors. *Curr Protoc Microbiol*. 2012;26(1): 14D.1.1–14D.1.21.

54. Gessler DJ, et al. Redirecting *N*-acetylaspartate metabolism in the central nervous system normalizes myelination and rescues Canavan disease. *JCI Insight*. 2017;2(3):e90807.
55. Wang H, et al. Widespread spinal cord transduction by intrathecal injection of rAAV delivers efficacious RNAi therapy for amyotrophic lateral sclerosis. *Hum Mol Genet*. 2014;23(3):668–681.